Apel, H., Hung, N. G., Thoss, H., Schöne, T. (2012): GPS buoys for stage monitoring of large rivers. - Journal of Hydrology, 412-413, 182-192

DOI: 10.1016/j.jhydrol.2011.07.043

# GPS buoys for stage monitoring of large rivers

H. Apel[a], N.G. Hung[a,b], H.Thoss[a], T. Schöne[c]

---

Heiko Apel, GFZ German Research Centre for Geoscience, Section 5.4 Hydrology, Telegrafenberg, 14473 Potsdam, Germany. (hapel@gfz-potsdam.de, +49 331 2881538, **corresponding author**)

Nguyen Nghia Hung, GFZ German Research Centre for Geoscience, Section 5.4 Hydrology, Telegrafenberg, 14473 Potsdam, Germany. (hung@gfz-potsdam.de, +49 331 2881555)

Heiko Thoss, GFZ German Research Centre for Geoscience, Section 5.4 Hydrology, Telegrafenberg, 14473 Potsdam, Germany. (thoss@gfz-potsdam.de, +49 331 2881544)

Tilo Schöne, GFZ German Research Centre for Geoscience, Section 1.2 Global Geomonitoring and Gravity Field, Telegrafenberg, 14473 Potsdam, Germany. (tschoene@gfz-potsdam.de, +49 331 2881739)

[a] GFZ German Research Centre for Geoscience, Section 5.4 Hydrology, Telegrafenberg, 14473 Potsdam, Germany

[b] Southern Institute of Water Resources Research, Ho Chi Minh City, Vietnam

[c] GFZ German Research Centre for Geoscience, Section 1.2 Global Geomonitoring and Gravity Field, Telegrafenberg, 14473 Potsdam, Germany

**Abstract**

Monitoring of river stages is one of the basic observations required for understanding catchment hydrology and hydraulic systems. There are numerous measurement techniques available for this purpose, but in case of large rivers technical as well as financial problems often restrict the use of traditional techniques, e.g. pressure probes or float gauges. We explored the potential of Global Navigation Satellite System (GNSS) based water level measurements for stage monitoring by developing small and easy to handle buoys equipped with high-quality geodetic GNSS receivers. The design of the buoys was particularly suited to the requirements of application in rivers, distinguishing them from typical wave rider buoys used in marine offshore applications. The advantages of buoys include the freedom of positioning and their quick and easy deployment. The developed buoys were tested in the Mekong Delta, Vietnam, at two different locations: on the Mekong river under high currents, and the second in a small nearby lake with hydraulic connections to a major channel with negligible currents. For this study, only data of the Global Positioning System (GPS) was collected and processed. Processing was undertaken in baseline mode using a nearby reference station and validated against standard pressure gauge data. The recorded stages proved to be of high quality (i.e. mean absolute error < 2 cm), thus potentially providing a useful resource for flood monitoring and modeling. In addition to the stage data, the results showed also the potential for monitoring position changes of the buoy and thus water movement. In the presented case study alternating currents caused by ocean tides could be detected, thus providing additional information about the hydraulic system. We conclude that the developed buoys add well to the existing hydrological monitoring pool and are a good option for the monitoring in rivers where traditional methods are technically difficult to deploy or too costly.

Keywords: GPS river buoy, GPS water elevation, hydrological monitoring, Mekong Delta

## 1. Introduction

In the past decade, monitoring marine water elevation using the Global Navigation Satellite System (GNSS) has been developed continuously and is now an accepted alternative to standard hydrometric procedures. Reported accuracies reach the sub-centimeter level [*Marshall and Denys*, 2008]. There are two main applications of using GNSS in marine applications, the first is the use in wave rider buoys to estimate 2-dimensional wave spectra, and the second application is the use in deriving well defined water level heights. The scope of this paper focuses on the latter application. In this type of application the buoys are equipped with a high-quality geodetic GNSS receiver. In previous works these buoys were applied in temporal campaign-like installations in coastal areas [*Watson et al.*, 2009], for tidal datum transfer [*Marshall and Denys*, 2008], for the calibration of satellite radar altimetry in short-term installations (e.g. Watson et al., 2003; *Schueler and Hein*, 2004; *Chen et al.*, 2004), or in permanent installations on the open ocean as part of the Indonesian Tsunami Warning System [*Schöne et al.*, 2011; *Schöne et al.*, 2003]. There are two main types of buoys, which can be differentiated into small and easy to handle buoys using, e.g., a life-saver as floatation device, and ruggedized large-scale buoys for application at the open ocean. The application of the small buoys is usually restricted to short duration because of power supply limitations, while the large-scale buoys are designed for autonomous long-term use [*Marshall and Denys*, 2008]. There is also a trade-off between handling and the momentum of the buoy. Small buoys are easy to handle and deploy but are limited to near-coastal installations and calm to moderate weather conditions. The large-scale buoys require large vessels and cranes for deployment due to their sheer dimensions and weights, but can be operated under severe weather conditions. For example, the buoys used in the German-Indonesian Tsunami Early Warning System (GITEWS) (*Schöne et al.*, 2011), are about 6 m high, 2.2 m in diameter and weight about 3 tons, but can be operated in storms reaching wind speeds of BF12. An overview of marine GNSS buoy designs is given in *Watson* (2005).

In contrast to marine sciences the use of GNSS techniques for water elevation measurement of rivers, especially for continuous monitoring, is practically unknown. The only notion of using the techniques was given by [*Moore et al.*, 2000], where laboratory experiments and a short term test of a GPS buoy on a river yielded promising results. To our knowledge, also industrial developments do not exist in this respect. The present study draws on these experiences of Moore et al. and aims at the development and testing of GNSS (GPS) buoys for continuous water level monitoring in rivers in order to explore the potential of this technology for hydrologists and hydraulic engineers. The following sections describe the development of the buoys according to the specific design criteria, the data processing and evaluation in detail.

## 2. Buoy development

The design of the buoys aimed at a maximum flexibility in selecting mooring options, i.e. it should be possible to fix them to another floating device as well as to a ground anchor without impairing the accuracy of the measurements. Therefore, the development of the buoys was guided by the following design criteria:

a) the buoy should have a minimal roll and pitch in various sea state conditions and should not submerge in high currents up to 3 m/s
b) size and weight should be small enough that the buoy can be handled by two to three persons from a small boat or vessel
c) the buoy should have an autonomous power supply sufficient for unrestricted continuous operation
d) data retrieval and GPS receiver control at the buoy should be possible during operation on water.

In order to meet design criteria a) the hull of the buoy was shaped similar to punt boats providing sufficient stability, i.e. minimum dipping and tilt and a stable distance of the antenna reference point (ARP) to the water surface, even under high currents. This feature distinguishes them from the mainly spherical shape of the small marine ("wave rider") buoys. This is of particular importance when the buoys are moored in a river with high or alternating currents, e.g. in flood situations. Under these conditions the current in combination with the vertical drag force component of the anchor chain would cause the spherical wave riders to dip and thus creating errors in the water elevation measurements. The extra buoyancy and the boat-like shape of the hull in combination with a frontal anchor point ensures minimum dipping of the buoy and, therefore, of the antenna position. Qualitative evidence of negligible dipping was gathered by observing the buoys in operation. However, experiments during the design of the buoy have shown that the buoy tilts slightly under different flow velocities, but the distance of the center point, where the antenna is fixed, to the water surface remains almost constant. By counterbalancing the frontal drag of the anchor chain with the weight of the battery in the rear, the buoy tilts around the center point. The tilt can be trimmed by variable anchor points at the buoy, which can be chosen according to the load of the buoy, the length of the anchor wire, and the water depth.

In order to reduce multipath effects, i.e. disturbing influences of backscattered GPS signals on the measurements, the solar panels are mounted horizontally and as low as possible. Also the use of a choke ring antenna aims at a minimization of multipath effects.

Figure 1 gives impressions of the buoys in operation and of their interior, while Fig. 2 illustrates the tethering. The dimensions of the buoy are 130x60x50 cm (length x width x height) with a volume of approximately 0.4 $m^3$. The hull is manufactured from aluminum alloy with a wide top lid for easy access to the buoys interior during maintenance on land. The buoy is equipped with a Topcon GB1000 GPS receiver and a CR-G3 choke ring antenna. The

distance of the ARP to the water surface is 30.5 cm, The power supply is ensured by 3 solar panels with a combined maximum power output of 65 Wp (Watt-peak), charging a 12V, 100 Ah Absorbed Glass Mat (AGM) battery through a charge control unit. The Topcon GB1000 features interface connectors for data access and control, which were extended to the hull of the buoy by water-proof connectors and are accessible without opening of the buoy (Fig. 1d). Remote data transfer is not implemented in the current design, but with the prospect of further development of the buoys and a potential operational use, this will be considered in future. With all components installed the buoys weight is approx. 50 kg, which can be reasonably handled by 2-4 persons. The dimension and weight also allow easy mooring of the buoys at the desired location via small vessels.

It should be noted, that, although the Topcon GB1000 tracks GPS and GLONASS, only GPS data was acquired to reduce the data volume to be stored at the buoy. For the same reason the sampling frequency of the buoy receivers was set to 0.5 Hz.

## 3. Study site

The developed buoys were tested in the Plain of Reeds of the Mekong Delta in Vietnam near the border to Cambodia. In the flat area of the Delta in Vietnam, numerous man-made channels exist in addition to the natural streams. Most of the rivers and channels are enclosed by dikes which, in combination with sluice gates and pumps, create a very complex hydraulic system. Due to the low-lying topography, the monitoring of water levels has to be accurate to a few centimeters, because small differences in water levels can cause considerably larger inundation areas. The delta is hydrologically characterized by two major aspects:

1. Pronounced low flow and flood seasons, where the flood season approximately ranging from end of July to November causes large inundations. At the study area, low

flow velocities are in the range of 0.6 m/s in the Mekong river, and rise to about 1.5 m/s during an average high flow (flood) . Flow velocities in the channels are considerably lower.

2. A strong tidal influence on the river water levels even more than 200 km upstream of the river mouths. A mixed tidal regime prevails with a period length of approximately 12 hours at the study site. Here the tidal regime is composed of a semi-diurnal signal from the South China Sea coming from South through the main river, and a diurnal signal from the Gulf of Thailand coming from West through the channels connecting the main river with the west-coast of the Mekong Delta. Other periodic signals of higher frequency do not exist (cf. Hung et al 2011 and results below).

Two prototypes of the buoys were deployed at different locations: The first buoy, B1, was deployed in the Mekong river (Tien river in Vietnamese), approximately 50 m off the river bank. This location can be regarded as a typical application site for the buoys, because the Mekong is about 1000 m wide at this location and the river banks are very unstable. A traditional gauging station would, therefore, require large construction works in order to guarantee reliable water level monitoring. However, a conventional absolute pressure probe has been installed at a bridge near a junction of a major channel to the Mekong close to the buoy location (Fig. 3). The probe is located 250 m away from the buoy. Buoy and pressure probe could not be installed at exactly the same location, because of the limitations of installing a gauging station on large rivers mentioned above and the restrictions of putting a buoy in a channel of limited with and with heavy ship traffic. The readings of the pressure probe (T1) were used for evaluating the quality of the data derived by the GPS buoy. . The pressure readings of T1 were collected in 15 min intervals and offline corrected for atmospheric air pressure measured 4 km away from the gauge location.

148 The second buoy, B2, is located in a small lake near a channel junction with a hydraulic
149 connection to a major channel. This location was selected because at the end of the flood
150 season often a reversal of the dominant flow direction can be observed. The initial plan was to
151 place the buoy directly at the channel junction in order to observe this phenomenon. However,
152 due to the limited channel width and the frequent ship traffic, the buoy had to be moved into
153 the lake. Figure 3 shows the positions of the buoys, the base station and the reference gauging
154 station T1.

155 Both buoys were deployed from June 2009 to start of September 2009.

156

157 **4. Data processing**

158 For the processing of kinematic GNSS buoy data two different approaches exist: precise point
159 positioning (PPP) and differential (baseline) solutions. To obtain elevation data, in this study
160 the more precise differential GPS solution computing the baseline from a reference station
161 was preferred to obtain the highest accuracy possible. For this purpose we installed a fixed
162 reference GPS station in the investigation area (Fig. 3). The antenna of the reference station
163 was fixed on the banister of the flat roof of a building, which is the highest in the vicinity.
164 However, there are some palm trees growing higher than the antenna nearby. On the roof
165 there is also a steel water tank, which is might deter the quality of the recorded GPS signals.
166 The base station was coordinated through a long-term static GPS observation and referenced
167 to UTM-coordinate system. The coordinates of the reference station antenna including
168 correction for geoid undulations [EIGEN5C mean tide geoid model, *Foerste et al.*, 2008] in
169 UTM Zone 48N coordinates are:

170 Northing [m]: 1182742.091

171 Easting [m]: 541464.977

Elevation [m]: 12.480

The baselines (distance) from the base station to the buoys are 8.1 km and 12.3 km to B1, and B2 respectively. GPS signals were recorded at 0.5 Hz at the buoys and at 1 Hz at the base station and stored in files with 0.5 Hz sampling interval covering 6 hour time slices. The frequency of 0.5 Hz sampling of the buoys was chosen as a compromise between accuracy of the GPS solution and data storage limitations of the GPS receiver in the buoys. Since sea state can be neglected, no aliasing is expected. With the given storage capacity of the receiver of 1 GB, data could be recorded for about 10 continuous days, after which the data had to be downloaded directly from the buoys. With the prospect of future remote data transfer, a higher GPS sampling rate can be implemented. The recorded data was processed with the Topcon Tools$^{TM}$ software in baseline method. The processing is done on the dual frequencies (L1 and L2) with a fixed ionosphere-free solution. The elevation cutoff angle was set to 10°.

The datum of T1 was also determined relatively to the base station by GPS using static records of 60 min occupation length, the vertical distance of GPS antenna to the pressure probe and the EIGNEN5C mean tide geoid model. The result of the processing of the buoy data is shown as “GPS raw data” in Figure 4. It is obvious that the data contains a considerable amount of noise and errors. The errors are mainly caused by incorrectly solved or unresolved cycle slips and possible multipath effects reducing the quality of the GPS signals. In order to assess the multipath effects we processed the recorded data with a different software (GAMIT) in baseline mode for a period of 8 days and with a PPP method, which available online (Automatic Precise Positioning Service – APPS, http://apps.gdgps.net/).. The PPP solution did not produce reasonable results, while GAMIT yields results comparable to the Topcon solution, suggesting multipath effects in the GPS data. An analysis of the multipath metrics of both buoy and base station GPS data revealed that the buoy behaves well showing only small multipath influence,. The base station data,

however, is impaired by multipath effects, most likely induced by reflections from the water tank and the nearby tree tops.

Nevertheless, the processed data show the same characteristics as the reference station T1 (Fig. 4), despite noise and unresolved cycle slips. We therefore developed a three step filtering procedure to extract the actual water level from the GPS data and to subsample the data from 2 sec intervals to 15 min intervals. For the given hydrological system, this data rate is still more than appropriate. The three steps of the filtering procedure illustrated in Fig. 5 are:

1. Automatic error detection and removal

For automatic detection of jumps and other significant errors in the 0.5 Hz time series we performed a wavelet analysis [*Torrence and Compo*, 1998] of 6 hour long time slices. Cycle slip related errors become apparent as significant signals in the wavelet power spectrum (Fig. 6, black encircled areas in middle panel) as well as in the average variance of signals over periods between 0 – 30 seconds (Fig. 6, lower panel). We used this information from the average variance for the detection of errors. The maximum period of the averaging window (30 seconds) is significantly smaller than any signal of interest in the given river system, especially from a hydrological point of view. All records of this scale averaged variance exceeding the 95% significance level compared to red noise (*Torrence and Compo*, 1998) were classified as high-frequency errors and are removed from the time series. This procedure is equivalent to a removal of significant high-frequencies in the wavelet power spectrum in Fig. 6b. The result of this operation is shown in the upper panel of Figure 6 in green along with the original data in red.

2. Intermediate data smoothing and subsampling

In a second step the GPS raw data was smoothed by a 15 minute average moving window. The smoothing was performed bi-directionally over the time series in order to prevent phase shifts. From this smoothed series individual records were subsampled at 15 minute intervals. The result of this operation is shown in Figure 4. After the subsampling all the obtained 15 min interval time series covering 6 hours each were concatenated to a water level series covering the whole observation period.

3. Frequency filtering of 15 min water level series

The 15 minute time series still contains noise, which has to be removed from the series. Therefore, another filtering was performed with frequency filters. Here we used again a wavelet analysis, but also a Butterworth digital filter was applied for comparison. Because the highest frequency with hydrological meaning in the water level series in this system is the tidal influence, we performed low pass filtering and removed periods below 6 hours corresponding to a half tidal cycle. The removal of the high-frequency signals is visualized in Figure 7 showing the power spectra before and after the frequency filtering. In the power spectrum of the filtered series no significant high-frequency signals are present, but the significant periods of 12 and 24 hours of the different tides are retained. Figure 4 shows the resulting water elevation time series of steps 2 and 3 for a number of days in August 2009 in comparison with the unfiltered data and the gauge readings of the nearby station T1.

## 5. Results and discussion

### 5.1 Data evaluation – water elevation

The final water level series of the buoys obtained by the filtering process was evaluated by comparison with records of the pressure gauge at T1. Figure 4 illustrates the differences exemplarily for some days in August 2009. It can be seen that there is no phase shift or bias

between the B1 and T1, and that the GPS derived water levels are of comparable accuracy to the gauge data. However, the tidal amplitude ranges are often slightly higher in the GPS water elevation time series compared to the pressure gauge. These features are characteristic for the whole time series of several months. The visual impression is corroborated by performance measures calculated for B1 referenced to T1 over a period of about 4 weeks. In the period 13.8.2009 – 9.9.2009 the bias between the gauge and buoy series is <1 mm, whereas the Root Mean Square Error (RMSE) and the Mean Absolute Error (MAE) indicating amplitude errors are 2.57 cm and 1.85 cm respectively. In the evaluation of these error figures, the scale error of the pressure probes has to be considered. The scale error of the pressure probe in the observed range a water depths is +/- 0.1%, which is equivalent to a maximum error of about +/- 6 mm water depths in the observed time period. I.e. the scale error of the gauge is considerably smaller than the observed amplitude errors, therefore other sources have to be investigated.

Table 1 lists possible error sources in the data processing and other relevant phenomena along with their influence on the processed time series. Given the fact that the hydraulic gradient between B1 and T1, and possible errors in the georeferencing of T1, i.e. the determination of the datum of the gauge, would only affect the bias, the errors in amplitude difference have to be attributed to the remaining sources. From those the amplitude dampening of the tidal signal in the channel compared to the Mekong is an aleatory error source that cannot be attributed to the method itself, in contrast to the possible errors caused by the buoy movement, the GPS signals and processing, and the filtering procedure. Due to the distance in location between B1 and T1, the lack of other reference data, missing movement sensors in the buoy and the complex hydraulic system it is hard to quantify the individual error contributions exactly. However, some estimations and sensitivity analysis were performed.

The maximum error introduced by the movement of the buoy (roll and tilt) can be estimated by the maximum expected tilt and roll angles. Since the buoy in its current development state does not contain a gyroscope, these angles can only be estimated from our observation of the buoy. We expect a maximum tilt and roll of 3°, which equates to a maximum elevation error of -5 mm given the vertical distance of the ARP to the water surface of 34 cm. This is comparable to the precision of the pressure gauge and is thus not considered further in the error analysis.

The heave of the buoy is likely to be influenced by the flow velocity of the river. In general, with higher flow velocities the buoy is likely to dip deeper compared to low flow velocities. As the buoy overestimates the tide induced amplitudes, this effect may contribute to the observed error. With high tide induced backwater effects, the flow velocity in the Mekong is lower compared to flow during low tide. Thus the tide induced amplitudes observed by the buoy may be amplified by this effect. However, at present it is not possible to quantify this effect due to missing additional instrumentation of the buoy quantifying the dip or other relevant information like direct flow velocity measurements of the Mekong.

The amplitude dampening can be estimated empirically from other gauging stations along the channel perpendicular to the Mekong river in which T1 is located. Comparing the amplitude readings of those stations, progressive amplitude dampening with increasing distance from the main river-channel junction becomes apparent. Based on these readings the amplitude dampening between B1 and T1 should be in the range of 0.5 – 1 cm. The effect of the filtering on the amplitude dampening was evaluated by a sensitivity analysis varying the width of the moving window in filtering step 2 and the cutoff period length of step 3 from 0 - 60 min, and 3 – 12 h respectively. The size of the moving window had only marginal effects on the amplitude after the frequency filtering of step 3. The RMSE of the reference period changed only in the range of +/-3 mm. However, the different cutoff periods, i.e. low-pass filter

thresholds used in the filtering (cf. Section 3, filter step 3), showed significant effects on the amplitude. This is shown in terms of performance measures in Fig. 8 and water elevations in Fig. 9. Fig. 8 shows that in fact the cutoff period of 6 hours yielded the best results in terms of RMSE, MAE and Nash-Sutcliffe efficiency [*Nash and Sutcliffe*, 1970]. Elongating or shortening the cutoff periods resulted in lower efficiency, while the bias remained constant. Figure 9 visualizes the filtering results with very short (1 h) and very long (12 h) cutoff periods on the water levels compared to the 6 h filtering and the reference gauging station T1. With only 1 h cutoff period a considerable amount of noise remains, while with 12 h the tidal amplitude is considerably dampened. This emphasizes the importance of selecting cutoff periods appropriate for the hydraulic system in the filtering process. It also shows that the results cannot be improved by filtering. This means in consequence that the observed differences in amplitude between buoy and reference are composed of the natural amplitude dampening in the channel, the quality and processing of the GPS signals, and to a lesser extend to the scale error of the pressure probes. A closer inspection of Fig. 4 shows that the most significant differences between B1 and T1 are associated with time periods of high noise in the GPS raw data (August 25$^{th}$, 12:00 – 24:00). Therefore, future work on improving the accuracy of the buoy data will focus on improving the floating stability of the buoy in water in order to reduce noise caused by unsteady floating, reducing the effects of multipath both at the buoys and the base station, and the GPS processing.

### 5.2 Data evaluation – buoy movement

In addition to the buoy derived altimetry the precise GPS positioning of the buoycan be used to calculate the horizontal velocity. Since the buoy is floating the position changes can be used as a proxy for detecting flow direction changes and determining the flow velocity for a short period during these changes. In our case study we calculated the movement velocity for buoy B2, because at its location near the channel junction far from the Mekong river, the buoy

318 can move more freely compared to B1, which position is dominated by the constant current of
319 the Mekong and therefore the buoy tether is taught for most of the deployment.. This is
320 illustrated by Figure 10 showing the tracks of B1 and B2 over the period June – November
321 2009, where the position is given relatively to the minimum easting and northing during this
322 period. At the location of B2, the tide induced water elevation changes cause alternating in-
323 and out-flowing currents in the small lake where the buoy is moored (Fig. 3). However, only
324 the dominant diurnal low tides significantly change the flow in and out of the lake, i.e.
325 outflow of the lake is associated with the diurnal low tide. Fig. 12 illustrates the different
326 amplitudes (water elevations) of the diurnal and semi-diurnal tides during low flow condition
327 in June 2009 as recorded by B2. Wind impacts play only a minor and temporary role in the
328 movement of the buoys, because no constant winds, both in direction and time, occur in the
329 area. Wind gusts are usually associated with heavy monsoonal storms of short duration.

330 The calculation of the movement velocities follows a similar procedure as the processing of
331 the water elevations described in section 5.1. Based on the 0.5 Hz GPS-derived time series,
332 the velocity is calculated from the position changes (projected x-y-coordinates). The resulting
333 velocity time series is processed analogously to the water elevations, i.e. corrected for
334 apparent cycle slips, smoothed by a 15 min average moving window and reduced to a 15 min
335 time series. This is again followed by a frequency filter removing periods smaller than 6
336 hours. Figure 11a shows the resulting 15 min time series. The series exhibits a tidal signal
337 that, in contrast to the water level, has only a single peak with a significant period of 1 day.
338 This is shown in the wavelet power spectrum in Fig. 11b and the global wavelet spectrum in
339 Fig. 11c. The comparison of the movement velocity and the acceleration calculated from the
340 velocities with the water elevations of B2 in Figure 12 shows that the acceleration of the buoy
341 is associated with the onset of the high tide after the lowest diurnal tide. This means that the
342 buoy is recording the in-flowing current. Over the next low tide, which is usually higher than
343 the lowest tide, the buoy does not accelerate as much, i.e. moves slowly without a distinct

direction. This is illustrated in Fig. 13. It shows that the buoy is moving around 6 a.m. local time daily into a distinct direction and back. This corresponds to the onset of the first daily high tide (Fig. 12). This evaluation of the buoy movement and its interpretation with respect to tidal influences on the hydraulic conditions in the lake of B2 illustrates the potential of the developed GPS buoys to detect and quantify valuable hydraulic information in addition to water elevations. This may be of particular significance in regions with low hydraulic gradients and changing flow patterns or alternating currents. However, it has to be noted that the anchored buoys cannot produce continuous time series of actual flow velocities, because their movement is restricted by the anchor chain. The emphasis here is rather on the quantification of the position change and acceleration as a short-term view of the flow velocities and the detection of flow direction changes and their timing. For continuous time series the buoys could be applied free floating. This, however, requires supervision to avoid collisions, grounding or even loss of the devices. Another option would be a flow rate sensor fixed underneath the buoy, whose readings can be corrected by velocities caused by buoy movement detected through the GPS records.

## 6. Conclusions

The developed GPS river buoys in combination with the proposed data processing chain proved to be capable of producing water elevation time series of acceptable accuracy compared to traditional pressure gauge data. The filtering procedure proved to be able to remove errors caused by unresolved cycle slips and noise caused by multipath effects at both buoy and reference station. The comparison of water elevations recorded at the gauge with elevations derived from the GPS buoy showed no time lag and bias between the buoy and the river gauge. However, the buoy apparently slightly overestimates the tide induced amplitudes. The causes for this effect remain equivocal, given the potential for different tidal dampening

at the buoy and gauge location, the influence of river flow velocities on the heave of the buoy, and possible remaining errors in the processing of the GPS data. However, at present the individual contribution of these error sources to the observed differences cannot be quantified. Therefore, future studies will focus on the improvement of the buoys floating dynamics in order to reduce the influence of wave action on the data quality. The buoy will also be equipped with sensors determining the dip in order to correct for possible influences of river flow velocities on the heave of the buoy. Other technical improvements will focus on the reduction of multipath effects on the GPS signals. This includes the use of ultra-slim solar panels and/or a higher position of the antenna- Also the position of the reference station will changed in order to reduce multipath at the GPS reference. Additionally the experimental setup will be changed in order to reduce the spatial distance between the buoy and the reference gauge. This should minimize the impact of natural hydraulic effects on the data evaluation and ease the error discussion of the water elevations derived by the buoy.

In addition to the water surface elevations, the GPS buoys provide information on water movement through evaluation of the horizontal coordinates recorded at high frequency. Utilizing these data the movement velocities as proxies for water flow velocities can be extracted in case the buoy changes position due to changing flow directions. This data has the potential to detect the timing of changes in flow patterns or alternating currents and to quantify the flow velocities shortly after the changes. When continuous time series of flow velocities are required, the buoys could be used in free floating mode, e.g. for the monitoring river flood peaks and flow velocities. However, it has to be noted that this application requires close supervision to avoid collision and other accidents.

Overall we conclude that even at the present development stage, the GPS river buoys provide a valuable tool that supplements the existing pool of hydrometric instruments. Given their

ease of deployment, they are well suited for water elevation monitoring of large rivers or lakes. The GPS buoy technology appears particularly useful in situations such as:

- where traditional gauging techniques are difficult or too costly to apply,
- whenever only a temporary gauging campaign covering, e.g., a single hydrological year is desired,
- or when additional information about flow direction or detection of changes in flow direction are sought after.

Another advantage of GPS technology is that height time series are derived in a geocentric reference frame, independent of subsidence or submerging of gauge constructions, which may occur at gauge constructions at river banks . Of course, it has to be ensured that no subsidence of the necessary reference station occurs. This can be achieved more easily compared to constructions along river banks, because the position of the reference station can be chosen freely at any point, i.e. a geologically stable position can be selected. However, it has to be kept in mind that a reference station needs to be established in the proximity of the buoy in order to obtain data with acceptable precision.

In perspective of operational use and improved handling of the buoys, their technical infrastructure will be extended by remote access and control, and online data transfer capabilities in the near future.

**Acknowledgements**

The presented work was developed within the frame of the WISDOM project: “Water related Information System for a sustainable Development of the Mekong Delta” (www.wisdom.caf.dlr.de). Funding by the German Ministry of Education and Research BMBF and the Vietnamese Ministry of Science and Technology is gratefully acknowledged.

We also thank Thees Behrens (Behrenswerft Hamburg, Germany) for his help in the design and testing of the buoys during construction.

## References

Chen, W., Hu, C., Li, Z., Chen, Y., Ding, X., Gao, S. Ji, S., 2004. Kinematic GPS Precise Point Positioning for Sea Level Monitoring with GPS Buoy, OSU Report 470, 2004

Foerste, C., Flechtner, F., Schmidt, R., Stubenvoll, R., Rothacher, M., Kusche, J., Neumayer, K.-H., Biancale, R., Lemoine, J.-M., Barthelmes, F., Bruinsma, J., König, R., Meyer, U., 2008. EIGEN-GL05C - A new global combined high-resolution GRACE-based gravity field model of the GFZ-GRGS cooperation, General Assembly European Geosciences Union. Geophysical Research Abstracts, Vol. 10, Abstract No. EGU2008-A-06944, Vienna, Austria (data available at http://icgem.gfz-potsdam.de/ICGEM/).

Hung, N.N. et al., 2011. Floodplain hydrology of the Mekong Delta, Vietnam. Hydrological Processes (http://onlinelibrary.wiley.com/doi/10.1002/hyp.8183/abstract).

Marshall, A., Denys, P., 2008. Water Level Measurement and Tidal Datum Transfer Using High Rate GPS Buoys, FIG (International Federation of Surveyors) Working Week 2008, 14-19 June, Stockholm, Sweden, pp. 15.

Moore, T., Zhang, K., Close, G., Moore, R., 2000. Real-Time River Level Monitoring Using GPS Heighting. GPS Solutions, 4(2): 63-67.

Nash, J.E., Sutcliffe, I.V., 1970. River flow forecasting through conceptual models. Part 1 - A discussion on principles. Journal of Hydrology, 10: 282-290.Schöne, T., Pandoe, W., Mudita, I., Roemer, S., Illigner, J., Zech, C., Galas, R., 2011. GPS water level measurements for Indonesia's Tsunami Early Warning System, NHESS GITEWS Special Publication (in print)

Schöne, T., Reigber, C., Braun, A., 2003. GPS Offshore Buoys and Continuous GPS Control of Tide Gauges. International Hydrographic Review, 4(3).

441 Schueler, T., Hein, G., 2004. ENVISAT Radar Altimeter Calibration with High-Sea GPS
442 Buoys, (http://forschung.unibw-
443 muenchen.de/papers/auv7mdtfu7nbtwdwvnftltrhcqpwkw.pdf)
444 Torrence, C., Compo, G.P., 1998. A practical guide to wavelet analysis. Bulletin of the
445 American Meteorological Society, 79(1): 61-78.
446 Watson, C., Coleman, R., Handsworth, R., 2009. Coastal Tide Gauge Calibration: A Case
447 Study at Macquarie Island Using GPS Buoy Techniques. Journal of Coastal Research,
448 24(4): 1071-1079.
449 Watson, C.S., 2005. Satellite altimeter calibration and validation using GPS buoys. University
450 of Tasmania, Hobart, 264 pp (http://eprints.utas.edu.au/254/).
451 Watson, C., Coleman, R., White, N., Church, J., Govind, R., 2003. Absolute Calibration of
452 TOPEX/Poseidon and Jason-1 Using GPS Buoys in Bass Strait, Australia - Special Issue:
453 Jason-1 Calibration/Validation. Marine Geodesy, 26(3): 285 - 304.
454

**Figure 1.** The developed GPS buoys “STREAM 1” in operation. a) buoy floating in Mekong river, b) interior of the buoy with GPS receiver and battery, c) solar panel and position lights, d) service interface underneath solar panel.

**Figure 2.** Sketch of the buoys tethering to a ground anchor.

**Figure 3.** Location of GPS buoys B1 and B2, the reference water level station T1, and the GPS reference station (source: Google Earth). Positioning of buoys (Lat/Long): B1: 10°46’08.55’’N / 105°21’23.08’’E, B2: 10°41’03.76’’N / 105°29’26.60’’E, reference station: 10°41’57,14’’N / 105°22’45,24’’E

**Figure 4.** Comparison of filtered GPS buoy water elevations B1 with water elevation of pressure gauge T1: processed unfiltered GPS data B1 (gray), 15 min moving window average smoothed series after error removal B1 (green), 15 min final frequency filtered water levels B1 (red), reference water level of T1 (blue).

**Figure 5.** Flow chart of the data processing

**Figure 6.** Wavelet analysis of processed unfiltered GPS data with 2 seconds time interval (cf. Fig. 4, gray lines). a) original series (blue), wavelet decomposed and reconstructed series for quality control of wavelet decomposition of time series (red, this is equal to the original series in case of optimal wavelet decomposition of the original series)), time series with errors removed (green); b) wavelet power spectrum of the raw GPS data series with significant signals encircled by black lines, white area below the cone of influence is not significant; c) global wavelet spectrum (blue solid) and significance level (dashed blue); d) average variance over periods from 0-30 seconds (blue solid) and significance level (blue dashed).

**Figure 7.** a) Long-term 15 min time series before (“errors removed”) and after low pass frequency filtering; b) wavelet power spectrum before low pass filter; c) wavelet power spectrum after low pass filter. The gray shaded areas indicate periods where no base stations

data were recorded due to hardware failures. Significant signals (at 95% significance level) in the power spectra are encircled in black. The low pass filter efficiently removed all high frequency noise as shown in c).

**Figure 8.** Performance criteria Root Mean Square error (RMSE), Mean absolute Error (MAE) and Nash-Sutcliffe efficiency (NSC) of comparison of B1 water elevations to T1 depending on different cutoff periods of the frequency filtering.

**Figure 9.** Effect of different cutoff periods (cp) used in the frequency filtering on B1 water elevations exemplarily for 1, 6, and 12 h cutoff periods, with 6 h being the best performing. Upper panel: direct comparison of the water level time series, lower panel: difference between reference T1 and B1.

**Figure 10.** Position plots of B1 and B2 for the period June 1$^{st}$ to November 30$^{th}$ with relative movement distances in east (x-axis) and north (y-axis) component.

**Figure 11.** Movement velocity of B1 for the period June 1$^{st}$ to July 16$^{th}$ (a); wavelet power spectrum of velocity time series before frequency filtering (b), black enclosed areas indicate significant signals; and c) global wavelet spectrum (blue) and significance level (black dashed)

**Figure 12.** Water elevation H, movement velocity v, and acceleration a of B2 for a number of consecutive days in June 2009, normalized to zero mean and standard deviation of 1 for direct comparison.

**Figure 13.** 3D position plot of B2 showing the acceleration of the buoy with the onset of low tide around 6 a.m. local time.

| Error source | Affecting |
|---|---|
| GPS signals & processing | Bias, Amplitude |
| Buoy dynamics (Heave and Tilt) | Amplitude |
| Buoy dynamics (Roll) | Bias |
| Filtering | Amplitude |
| Amplitude dampening in channel | Amplitude |
| Georeferencing of T1 | Bias |
| Hydraulic gradient B1 to T1 | Bias |

**Table 1.** Possible error sources associated to water elevations derived from buoy B1

Figure 1

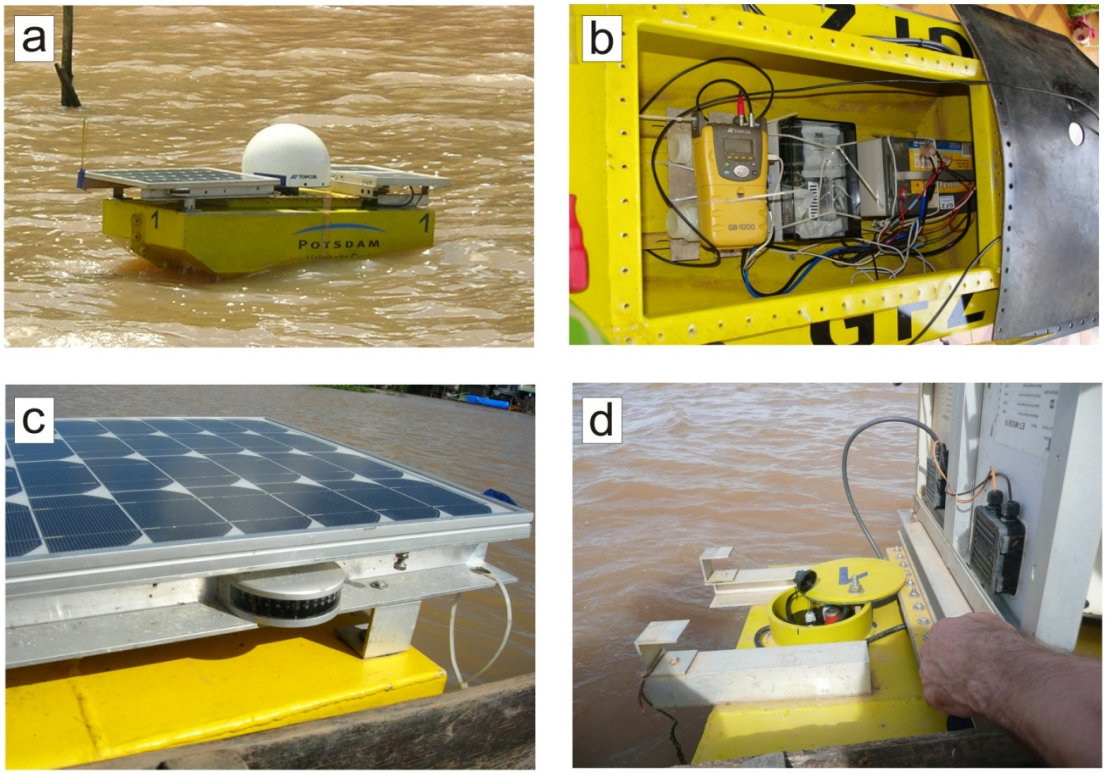

Figure 2

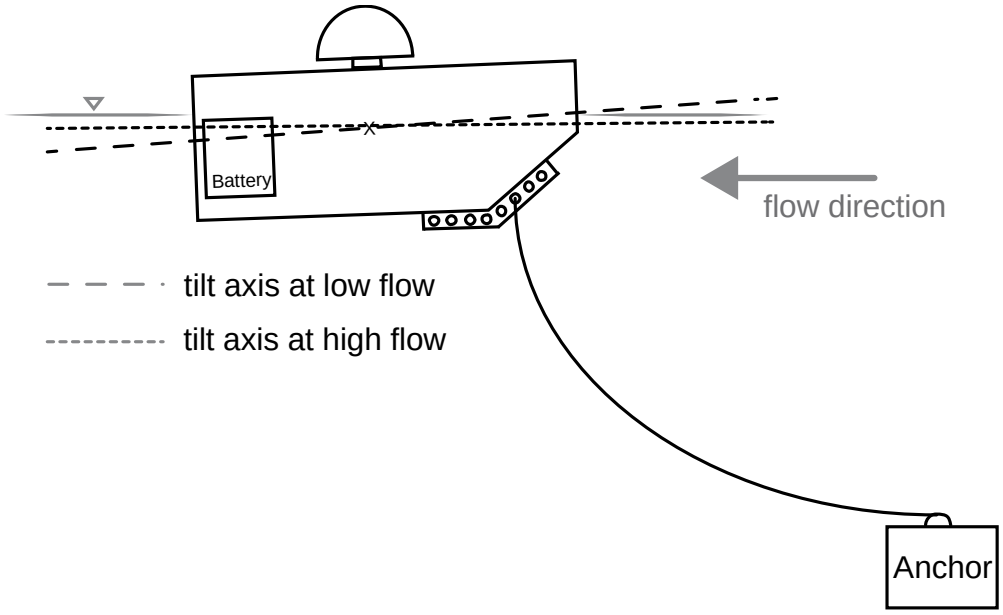
Battery
flow direction
tilt axis at low flow
tilt axis at high flow
Anchor

Figure 3

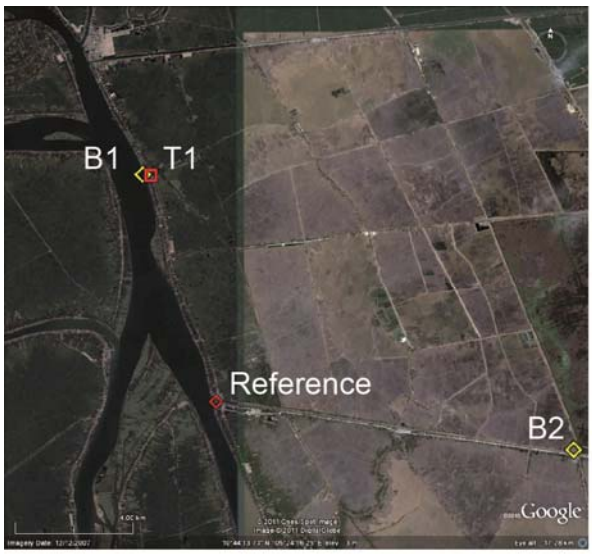
B1
T1
Reference
B2
Google


Reference
Google


B1
T1
Google


B2
Google

Figure 4

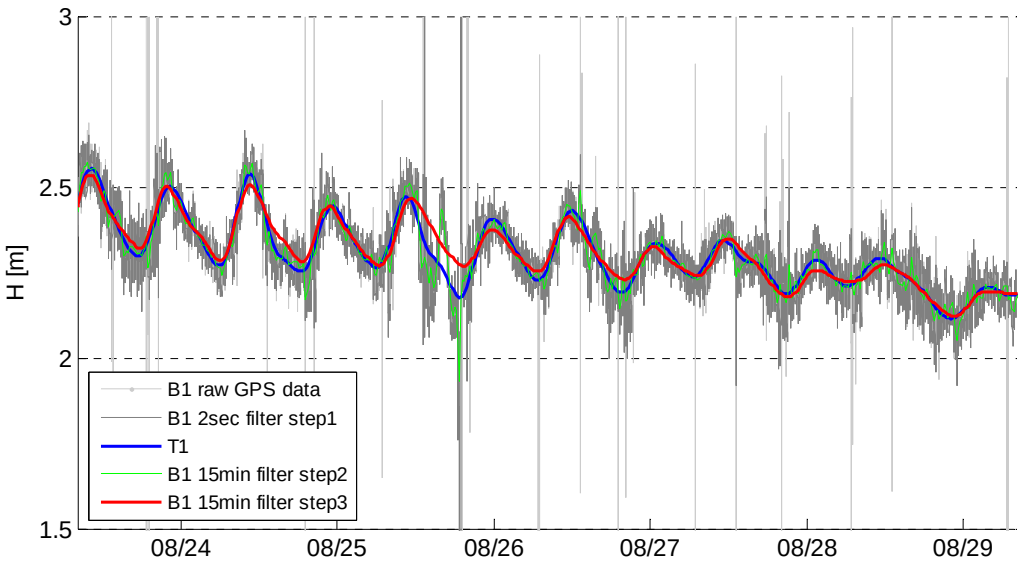
3
2.5
2
1.5
H [m]
B1 raw GPS data
B1 2sec filter step1
T1
B1 15min filter step2
B1 15min filter step3
08/24
08/25
08/26
08/27
08/28
08/29

Figure 5

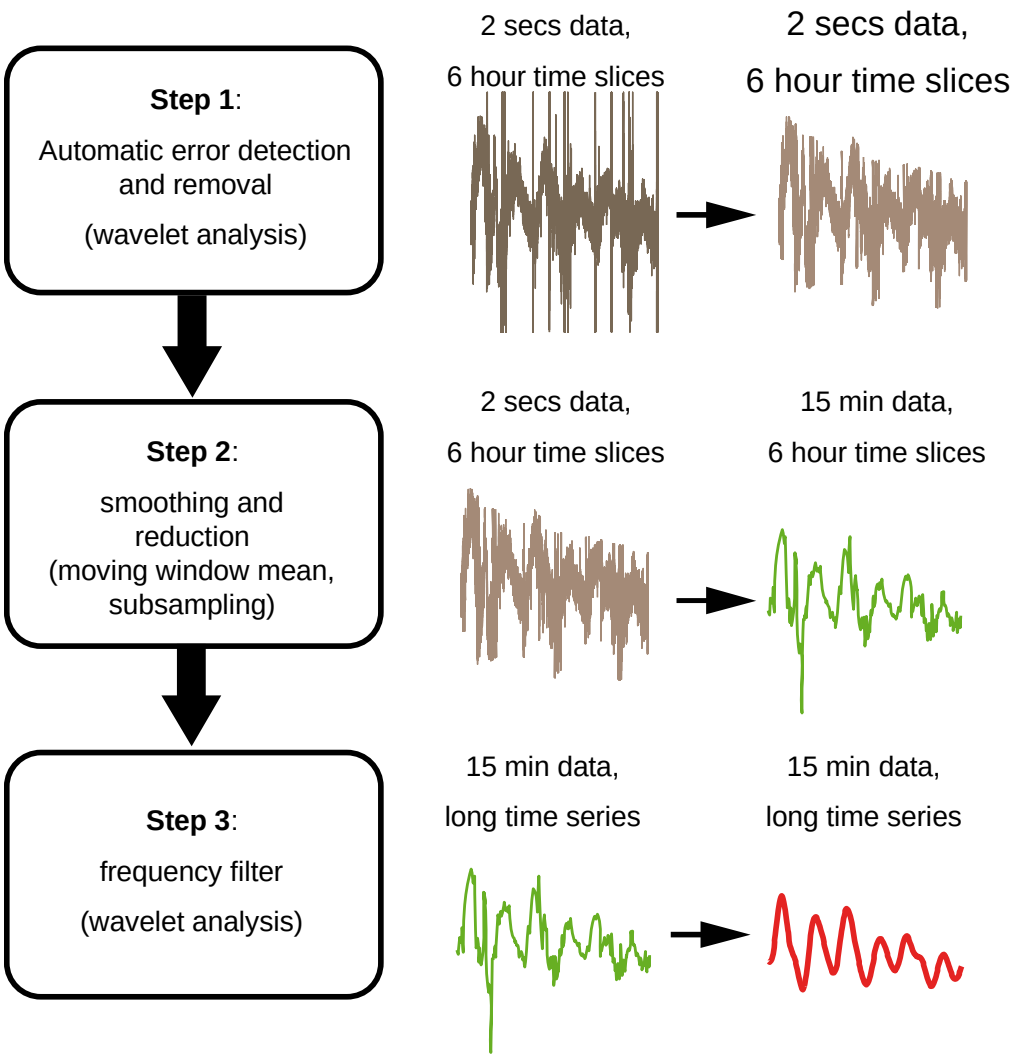
Step 1:
Automatic error detection and removal
(wavelet analysis)
Step 2:
smoothing and reduction
(moving window mean, subsampling)
Step 3:
frequency filter
(wavelet analysis)
2 secs data,
6 hour time slices
2 secs data,
6 hour time slices
2 secs data,
6 hour time slices
15 min data,
6 hour time slices
15 min data,
long time series
15 min data,
long time series

Figure 6

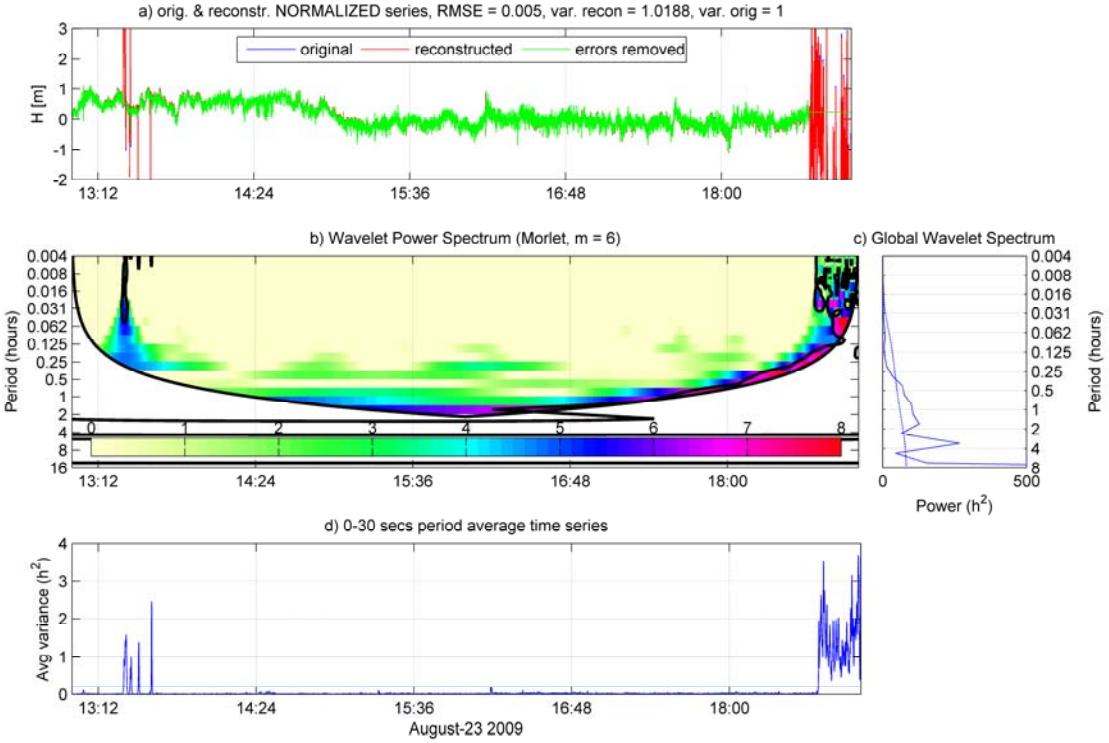
a) orig. & reconstr. NORMALIZED series, RMSE = 0.005, var. recon = 1.0188, var. orig = 1
original
reconstructed
errors removed
H [m]
13:12
14:24
15:36
16:48
18:00
b) Wavelet Power Spectrum (Morlet, m = 6)
c) Global Wavelet Spectrum
Period (hours)
Power (h2)
d) 0-30 secs period average time series
Avg variance (h2)
August-23 2009

Figure 7

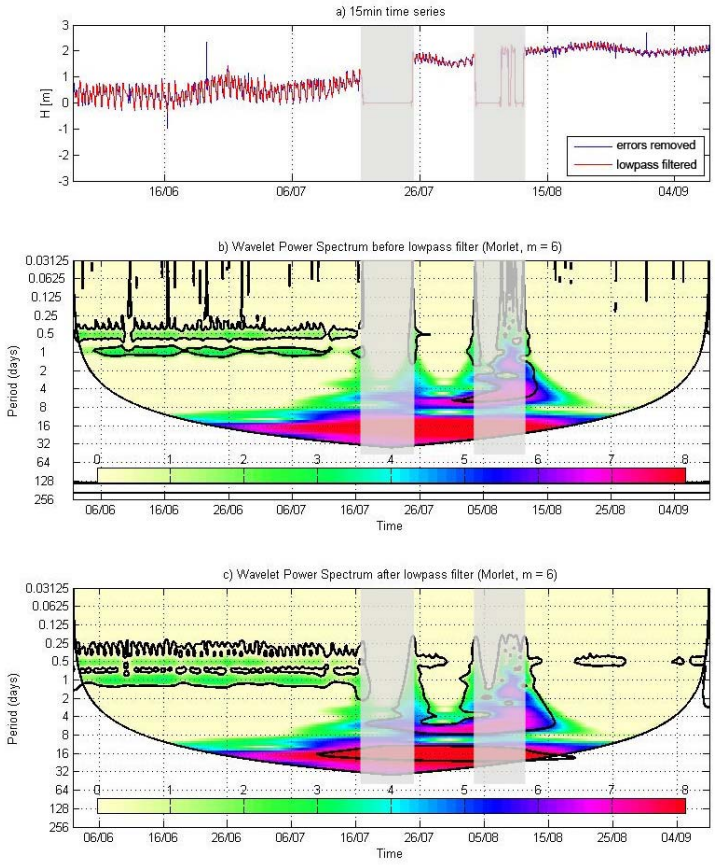
a) 15min time series
H [m]
errors removed
lowpass filtered
16/06
06/07
26/07
15/08
04/09
b) Wavelet Power Spectrum before lowpass filter (Morlet, m = 6)
Period (days)
Time
c) Wavelet Power Spectrum after lowpass filter (Morlet, m = 6)
Period (days)
Time

Figure 8

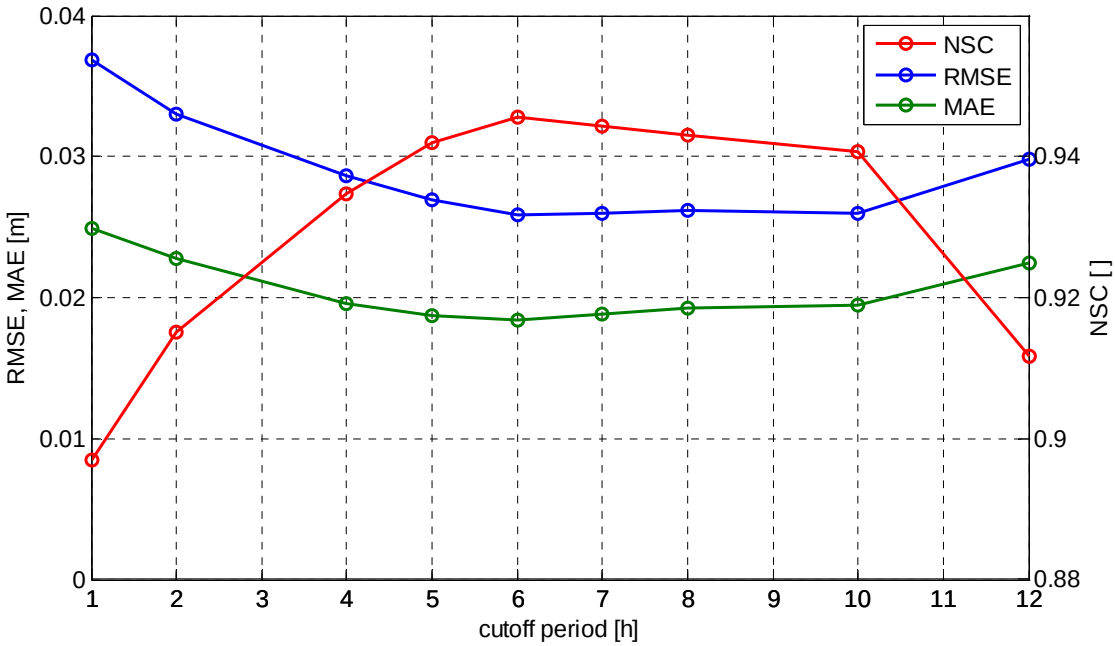
NSC
RMSE
MAE
RMSE, MAE [m]
NSC [ ]
cutoff period [h]
0.04
0.03
0.02
0.01
0
0.94
0.92
0.9
0.88
1
2
3
4
5
6
7
8
9
10
11
12

Figure 9

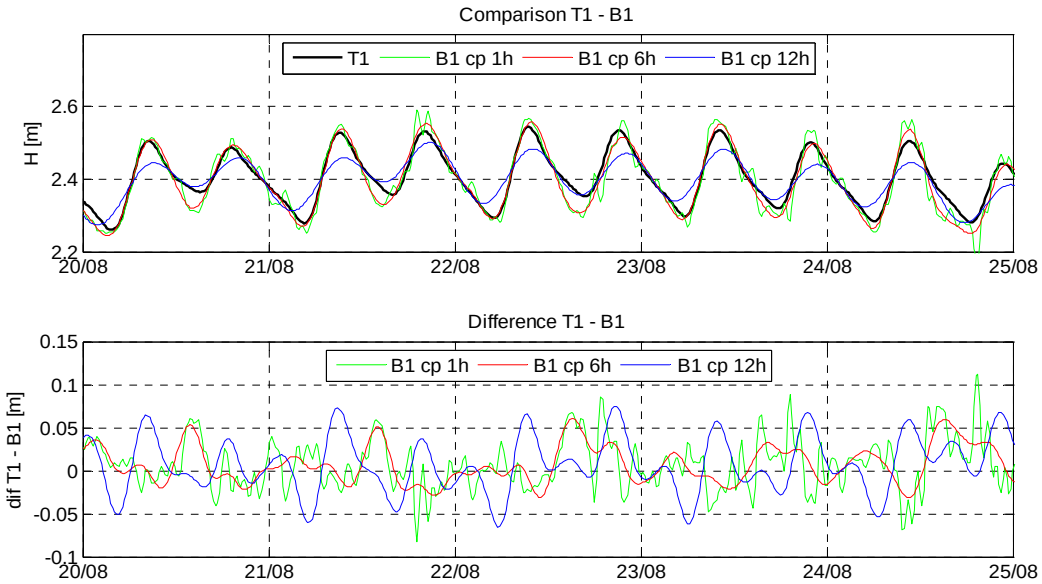
Comparison T1 - B1
T1
B1 cp 1h
B1 cp 6h
B1 cp 12h
H [m]
2.6
2.4
2.2
20/08
21/08
22/08
23/08
24/08
25/08
Difference T1 - B1
B1 cp 1h
B1 cp 6h
B1 cp 12h
dif T1 - B1 [m]
0.15
0.1
0.05
0
-0.05
-0.1
20/08
21/08
22/08
23/08
24/08
25/08

Figure 10

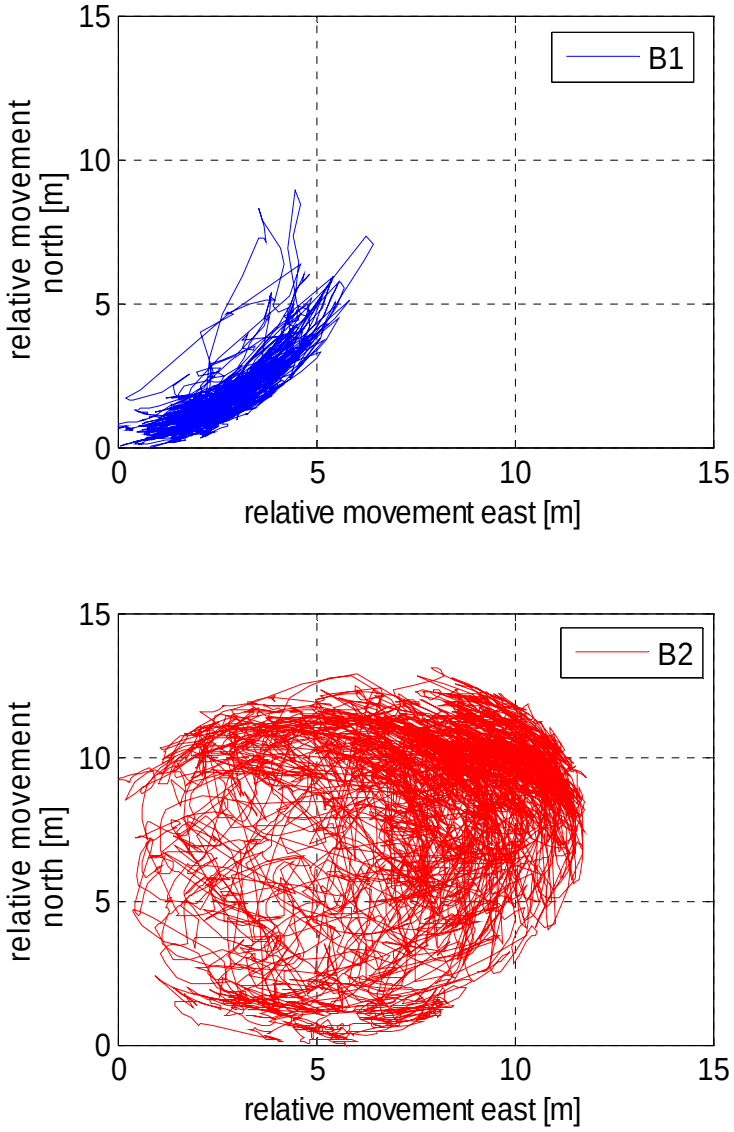
B1
relative movement north [m]
relative movement east [m]
0
5
10
15
B2
relative movement north [m]
relative movement east [m]

Figure

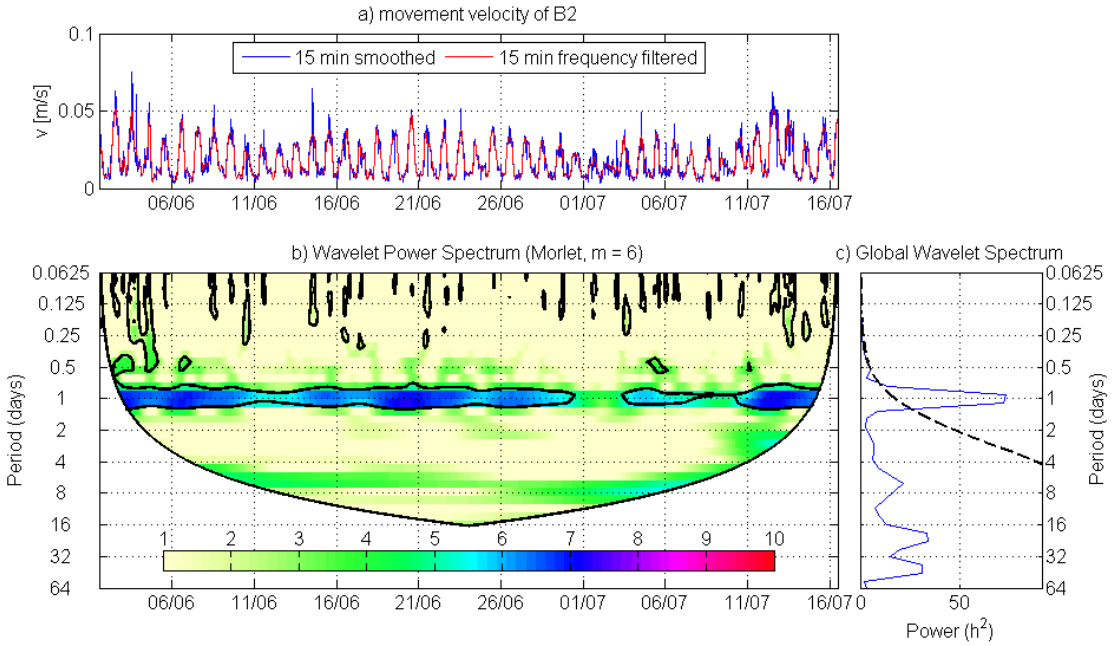
a) movement velocity of B2
15 min smoothed
15 min frequency filtered
v [m/s]
0.1
0.05
0
06/06
11/06
16/06
21/06
26/06
01/07
06/07
11/07
16/07
b) Wavelet Power Spectrum (Morlet, m = 6)
c) Global Wavelet Spectrum
Period (days)
0.0625
0.125
0.25
0.5
1
2
4
8
16
32
64
1
2
3
4
5
6
7
8
9
10
0
50
Power (h2)

11

Figure 12

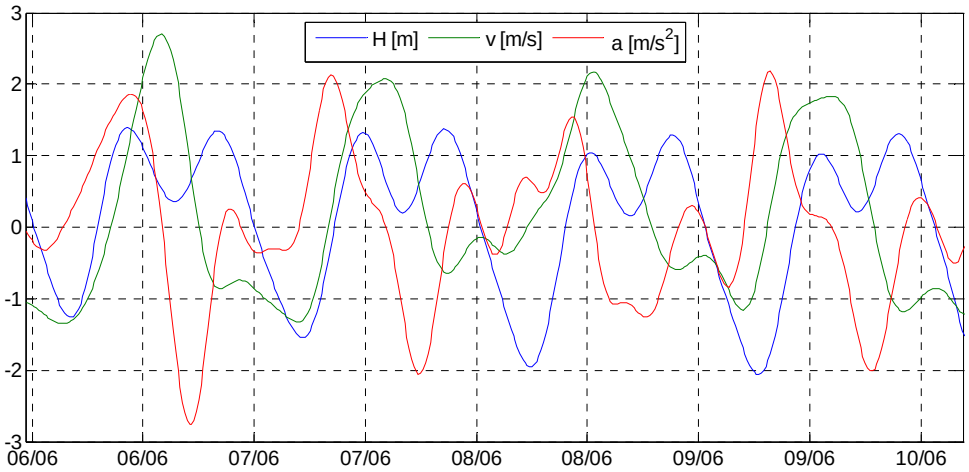
H [m]
v [m/s]
a [m/s$^2$]
3
2
1
0
-1
-2
-3
06/06
06/06
07/06
07/06
08/06
08/06
09/06
09/06
10/06

Figure 13

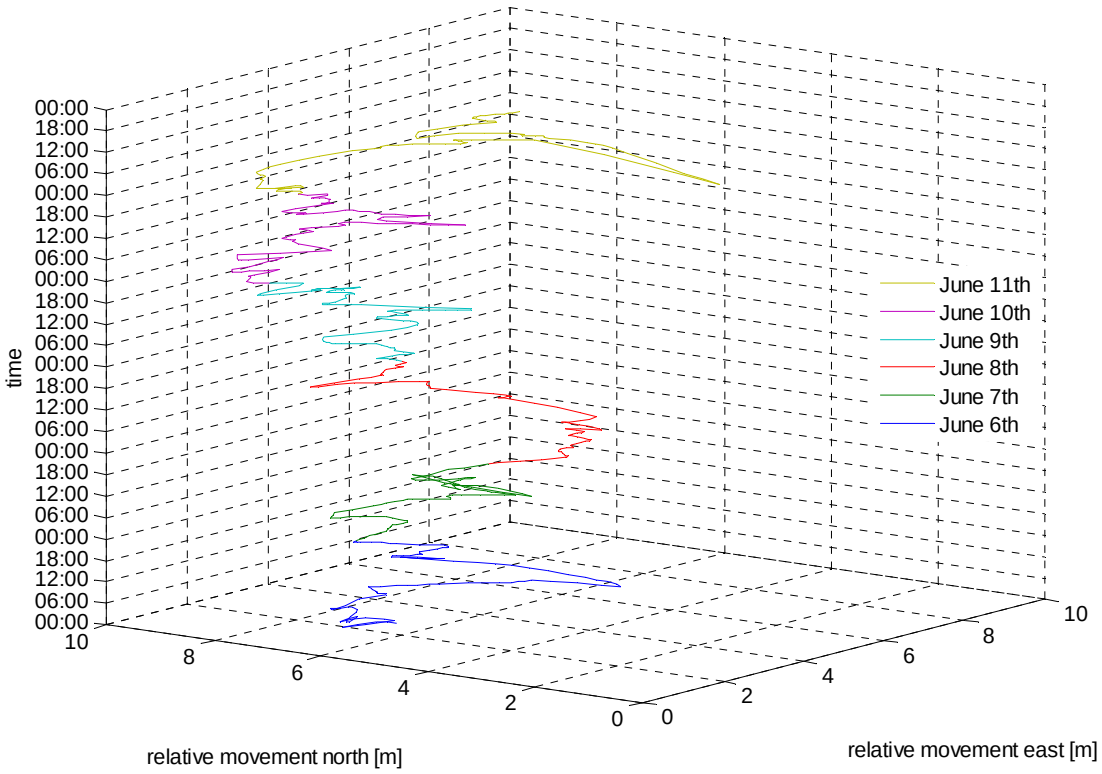
time
00:00
18:00
12:00
06:00
relative movement north [m]
relative movement east [m]
June 11th
June 10th
June 9th
June 8th
June 7th
June 6th